CrossMark

ORIGINAL RESEARCH

Polyvinylidene fluoride (PVDF)/polyacrylonitrile (PAN)/carbon nanotube nanocomposites for energy storage and conversion

Salem M. Aqeel[1,2] · Zhongyuan Huang[1,3] · Jonathan Walton[4] · Christopher Baker[4] · D'Lauren Falkner[1] · Zhen Liu[4] · Zhe Wang[1]

Abstract Polyvinylidene fluoride (PVDF)/polyacrilonitrile (PAN)/multiwalled carbon nanotubes functionalized COOH (MWCNTs-COOH) nanocomposites with different contents of MWCNTs were fabricated by using electrospinning and solution cast methods. The interaction of the MWCNTs with the polymer blend was confirmed by a Fourier transform infrared (FTIR) spectroscopy study. The dispersion of the MWCNTs in the polymer blend was studied by scanning electron microscopy. The dispersion of the MWCNTs in the polymer matrix at different compositions has been examined by using scanning electron microscopy (SEM). Both individual and agglomerations of MWCNTs were evident. Multiwalled carbon nanotubes are capable of enhancing the impedance and electrical conductivity of PVDF-PAN/MWCNTs in a wide frequency range at different temperatures. Nanocomposites based on PVDF/PAN and MWCNTs as fillers show a significant enhancement in the electrical conductivity as a function of temperature. In addition, PVDF/PAN with 5.58 wt.% of MWCNTs has a much higher specific energy (129.7Wh/kg) compared to that of PVDF/PAN (15.57 Wh/kg).The results reveal that PVDF/PAN/MWCNTs composites have potential applications for nanogenerators, organic semiconductors, transducers, and electrical energy storage.

Salem M. Aqeel and Zhongyuan Huang contributed equally to this work.

✉ Zhen Liu
zliu@frostburg.edu

✉ Zhe Wang
zwang@xula.edu

[1] Chemistry Department, Xavier University of Louisiana, New Orleans, LA 70125, USA

[2] Department of Chemistry, Faculty of Applied Science, Thamar University, P. O. Box 87246, Thamar, Yemen

[3] College of Chemistry and Chemical Engineering, Xinyang Normal University, Xinyang 464000, China

[4] Department of Physics and Engineering, Frostburg State University, Frostburg, MD 21532-2303, USA

1 Introduction

Polymer nanocomposites containing carbon nanotubes (CNTs) have generated extensive interest due to their electrical, physical, and mechanical properties. The nano-structural elements can be used as nano-fillers and nano-reinforcements of advanced composite materials to improve the mechanical, thermal, and impact-resistance properties [1–10]. Polyvinylidene fluoride (PVDF) and polyacrylonitrile (PAN) independently have useful characteristics as the important polymers in nanocomposites. It was determined that PAN has good process ability, flame resistance, resistance to oxidative degradation, and electrochemical stability. PAN also has a high oxidative stabilization even at high temperature [11]. Moreover, PAN could provide a few important characteristics towards polymer electrolytes which could not be derived from PVDF [12]. PVDF has been extensively studied as an important crystalline polymer for a broad range of applications, including, but not limited to, transducers [13], non-volatile memories [14, 15], and electrical energy storage [16, 17].

Nanocomposites, based on PVDF, PAN, and multiwalled nanotubes (MWCNTs), have been under investigation recently. CNTs could improve thermal stability and Young's modulus of PAN/SWCNTs nanofibers [18, 19]. As widely used dielectric material, the effect of CNTs on the electric properties of PVDF and PAN has yet to be understood fully. The nanofibers of PAN/CNTs revealed a significant improvement

in mechanical properties and thermal stability [18]. It has been shown that significant interactions occur between PAN chains and CNTs, which lead to higher direction of PAN chains during the heating process [20].

In order to obtain the consistent and uniform electric properties in one dimension, well-aligned and dispersed CNTs were desired in the host polymer. Electrospinning is a simple and low-cost method which could make CNTs embedded in a host, formed as a non-woven web [5, 21–23]. The performance of CNTs prepared using this method relies on the distribution of fibers within. It was discovered that in the electrospinning process, CNTs could be aligned along the fiber axis. A high voltage was used in this technique to create an electrically charged jet of polymer solution or melt. The electric field reached a critical value at which the repulsive electric force overcame the surface tension of the polymer solution. The polymer solution was ejected from the tip to a collector. While traveling to the collector, the solution jet solidified or dried due to the fast evaporation of the solvent and was deposited on a collector to leave a polymer fiber [24–28].

In this study, PVDF-PAN/MWCNTs copolymers with different content of MWCNTs were fabricated through electrospinning and the solution cast method to obtain new organic semiconductor composites. Their electrical conduction mechanisms are explained by a wide study of temperature dependence of conductivity in the frequency range of 0.5 to 10^4 Hz. Its relationship with blend ratios was investigated by morphology and Fourier transform infrared (FTIR).

2 Experimental

PVDF, with an average molecular weight of 2.75×10^5 g/mol, and PAN, with a molecular weight of 1.50×10^5 g/mol, were obtained from Sigma-Aldrich Co. Dimethylformamide (DMF) was obtained from VWR International LLC. Multiwalled carbon nanotubes (MWCNTs-COOH) with a diameter of 10 nm, length from 10 to 30 μm, and content of –COOH 1.9–2.1 wt.% was supplied by Nanostructured & Amorphous Materials, Inc., USA. The blends were prepared by using electrospinning and the solution cast method in DMF. PVDF-PAN-MWCNTs blended with different weight percent ratios and dispersed in DMF. The solutions were sonicated and stirred, before being poured into glass dishes. They evaporated slowly at room temperature and dried under a vacuum. The solid films continued to dry under the vacuum to remove residual solvent. The electrospinning setup consisted of a plastic syringe (5 mL) and a steel needle. The needle connected to a high-voltage power supply. An automatic voltage regulator was attached to the power supply to produce uniform voltages. The fiber deposited on an Al sheet on the grounded electrodes, both as a flat sheet and on a rotating drum. Polymer nanocomposites were electrospun at 15 kV,

with capillary-screen distances of 10 cm and flow rates of 2.5 ml/h.

For the characterization of the samples, a Fourier transform infrared spectrometry (FTIR, Varian 3100) was carried out at room temperature. The morphology of the composite was characterized by scanning electron microscopy (SEM) (JSM-6510GS from JEOL), operating with an accelerating voltage of 20 kV.

After drying, the polymer nanocomposites (prepared by electrospinning and the solution cast method) with dimensions 12 mm × 12 mm were sputtered, coated with gold, and sandwiched between two gold plates. The electrical measurements were performed by using a VersaStat MC.station (PrincetonApplied Research Inc, USA) at a frequency range from 0.5 Hz to 1×10^4 Hz.

3 Results and discussion

The effect of nanoparticles on morphology and properties of polymer blends have attracted great interest because of the improved physical properties as compared with unmodified polymers. The SEM image of the PVDF/PAN/MWCNTs
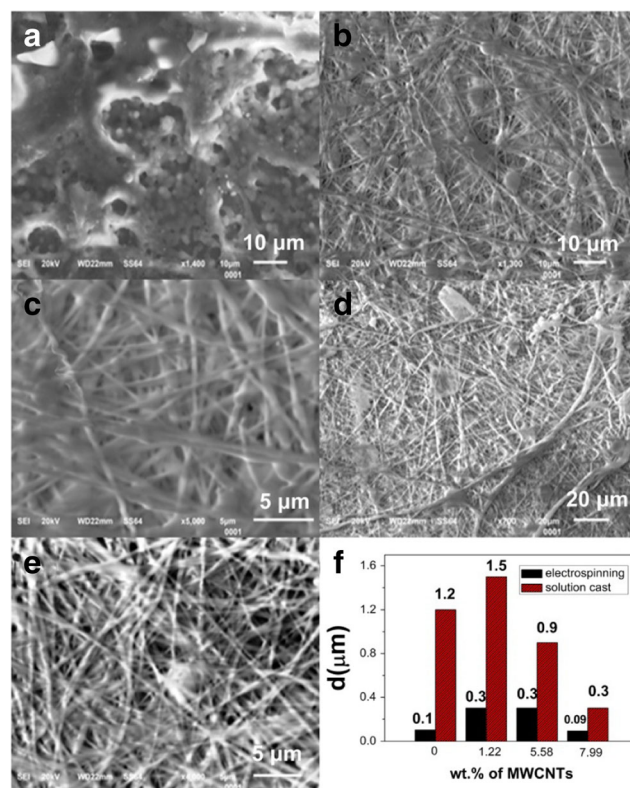
Fig. 1 SEM images of the PVDF-PAN-MWCNTs-COOH composites prepared by solution cast method with 5.47 wt.%. of MWCNTs (**a**) and electrospinning method with 5.58 wt.%. of MWCNTs (**b**, **c**) and with 7.99 wt.%. of MWCNTs (**d**, **e**). **f** The size distribution of PVDF-PAN-MWCNTs-COOH fibers prepared by solution cast and electrospinning methods as a function of MWCNTs content
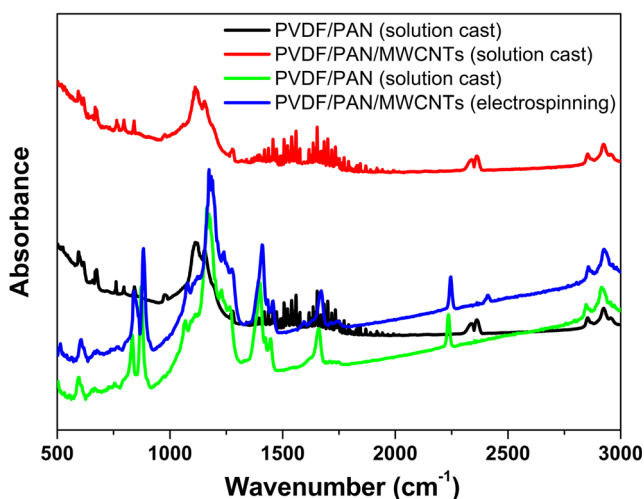
composites prepared by solution cast method is given in Fig. 1a, which clearly shows highly entangled network-like structure of MWCNTs. The percolated MWCNTs with network structure and good dispersion are evident in PVDF/PAN-MWCNTs composites with 5.47 wt.% of MWCNTs. The functionalization of MWCNTs increases the compatibility of MWCNTs with PVDF/PAN so as to improve the dispersion of MWCNTs in polymer nanocomposites. Compared with the polymer/MWCNTs prepared via an in situ bulk polymerization, the solvent cast film shows a better nanoscopic dispersion of MWCNTs [29].

The PVDF-PAN/MWCNTs fibers interconnected with a large number in different sizes have non-woven structure. The interconnections of the PVDF/PAN/MWCNTs fibers increased as the mass content of MWCNTs in the composite increased. The interconnected network morphology was expected to probable molecular level interactions between C–F (in PVDF) and –CN (in PAN). These molecular interactions induce the phase mixing between PVDF and PAN [30, 31]. Figure 1f summarized the size distribution of the fiber's diameters processed from different concentrations of MWCNTs in PVDF-PAN. It was observed that the diameter of the fibers prepared by the solution cast method was mainly in the range of 0.3–1.5 μm, while the fibers prepared by the electrospinning method was mainly in 0.09–0.3 μm. Fiber diameter clearly decreased when wt.% of MWCNTs increased from 1.22 to 7.99 wt.% in PVDF-PAN/MWCNT nanocomposites prepared by the electrospining method due to the higher charge density of the electrified jet forming more uniform and much thinner fibers from the polymer solutions containing well-dispersed MWCNTs [32]. The specific surface area of the MWCNTs was higher than that of PVDF-PAN. With a higher specific surface area, the electrostatic interaction of functional groups on the MWCNTs can act as nucleating agents in the electrospinning process of polymer

nanocomposites. This leads to higher charge density of the electrified jet, forming uniform and much thinner fibers from the polymer solutions containing well-dispersed MWCNTs.

In order to understand how the interaction improves the compatibility of the polymer nanocomposite, FTIR analysis was performed. Figure 2 shows the FTIR spectra of PVDF-PAN-MWCNTs prepared by electrospinning and the solution cast method. The FTIR spectra of MWCNTs shows major peaks, located at 2880, 2361–2364, 1700, and 1560 cm^{-1}. The peaks at 2880 and 2361–2364 cm^{-1} are attributed to H–C stretch modes of H–C = O in the carboxyl group and O–H stretch from strongly hydrogen-bonded –COOH respectively [33]. The peaks at 1700 cm^{-1} and 1560 cm^{-1} are corresponded to carbonyl groups of COOH and the C = C stretch of the COOH in MWCNTs respectively [33]. Characteristic peak at 2214 cm^{-1} is due to the stretching vibration of the cyano group (–CN), 1454 cm^{-1} for (–CH$_3$) and 1373 cm^{-1} (–CH$_2$), which can be observed in PAN [34]. In addition, FTIR spectra of composites show bands around 1140–1180 cm^{-1} and 1411–1419 cm^{-1}, which are corresponding to the CF$_2$ bending and CH$_2$ stretching mode [35], respectively. FTIR results indicate that there are molecular level interactions between the two polymers in the nanofibers. These spectral features give a hint for probable phase mixing between PVDF and PAN.

As shown in Fig. 3, the characteristic peaks of the α-phase (non-polar phase) are obtained at 615, 765, and 790 cm^{-1}, while the characteristic peaks of the β-phase (polar phase) are observed at 510, 840 and 1270 cm^{-1}. The occurrence of weak bands for composites prepared by solution cast at 615, 765, and 790 cm^{-1} indicate the presence of a small amount of the α-phase. This is observed by comparing it with polymer nanocomposites prepared by the electrospinning method. It also shows that the β-phase will increase while the α-phase decrease when there is an increase in MWCNTs content.

Fig. 2 FTIR spectra of PVDF/PAN and PVDF-PAN/MWCNTs composites prepared by solution cast and electrospinning methods
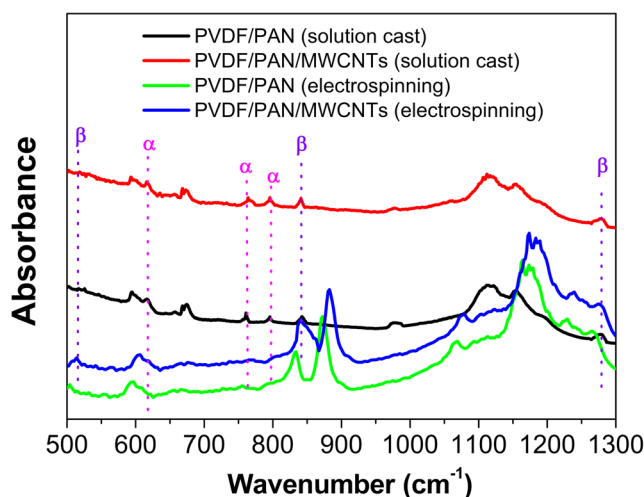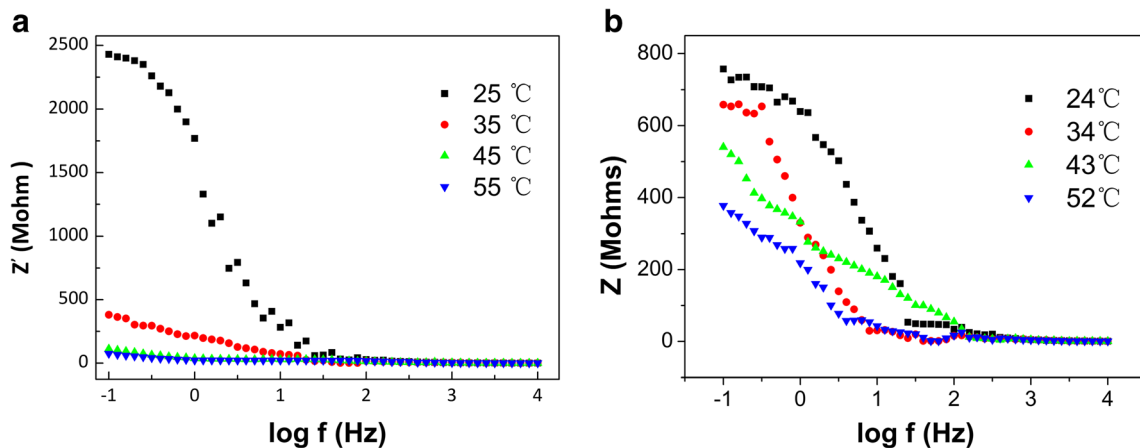

Fig. 3 FTIR spectra, α and β formation of PVDF/PAN, and PVDF-PAN/MWCNTs nanocomposites prepared by solution cast and electrospinning methods
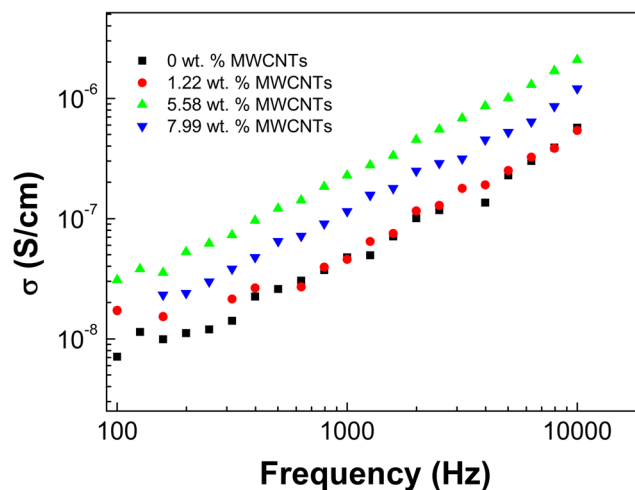
The intensities of the β-phase became stronger, while the bands of the α-phase became weaker, suggesting that the α-phase is progressively replaced by the β-phase [36, 37]. It is well known that the specific surface area of MWCNTs is higher than that of PVDF.

This allowed MWCNTs to act as nucleating agents in the initial crystallization process of PVDF, leading to a high degree of crystallinity [38]. Under the external electric field in electrospinning, MWCNTs can produce inductive charges on the surface, thus lead to a greater Coulomb force during the electrospinning processes. The Coulomb force would then attract part of PVDF chains to the MWCNTs surface. The β-phase PVDF would be derivated near the interface during this process. By the electrostatic interaction of functional groups on the MWCNTs, which then act as nucleating agents with the polar-CF_2, the PVDF chain will have the zig-zag (T T T T conformation) of the β-phase, instead of the coiled α-phase (TGTG conformation). The characteristic of the γ-phase is observed at 1233 cm^{-1}, and can be obtained from strongly polar solvents such as N,N-dimethylformamide (DMF). In the electrospinning process, piezoelectric (β and γ) phases could still be induced via the dipolar/ hydrogen interactions between the local polar structure in the crystalline PAN and PVDF [39]. This result is consistent with PVDF/nylon 11 blends [40].

Impedance spectroscopy measurements of the electrical properties for PVDF-PAN/MWCNTs composites were performed with different concentrations of MWCNTs. They had a temperature range of 297–327 K at frequencies between 0.5 and 10^4 Hz. Figure 4a, b shows the variation of impedance (Z) for the PVDF-PAN/MWCNTs (prepared by electrospinning and solution cast methods with different concentrations of MWCNTs) as a function of frequency at different temperatures. The magnitudes of Z decreased at lower

Fig. 5 The conductivity for the PVDF-PAN/MWCNTs (prepared by the electrospinning method) as a function of frequency

frequencies with increased temperature. At high frequencies, the value of Z merged for all the temperatures of the sample.

The frequency-dependent conductivity of the polymer nanocomposite is described by the Eqs. [41, 42]:

$$\sigma(\omega) = \sigma_{dc} + A\omega^n \quad (1)$$

where A is the material parameter, n is the frequency exponent in the range of $0 \leq n \leq 1$, σ_{dc} is dc conductivity, and ω is the angular frequency. The conductivities of PVDF-PAN/MWCNTs nanocomposites with different MWCNTs concentrations as a function of the frequency are presented in Fig.5. The conductivity of PVDF/PAN films showed typical frequency dependence due to the low conductivity of these polymers. With the addition of 1.2 wt.% of MWCNTs into the polymer, the frequency-dependent AC conductivity with the comparable value to that of PVDF/PAN blend was still preserved. A significant change of the conductivity occurred when the MWCNTs content of the polymer rose from 1.2 to

Fig. 4 The impedance (Z) for the PVDF-PAN/MWCNTs prepared by electrospinning method (**a**) and PVDF-PAN/MWCNTs prepared by solution cast method (**b**) as a function of frequency

5.5 wt.%. The frequency-dependent conductivity shows two regions. The plateau region corresponds to the frequency-independent dc conductivity (i.e., σ_{dc}) and the dispersive region corresponds to the frequency-dependent part [43]. It was confirmed by a typical fit of the above equation to the experimental data shown in Fig. 5 that the value of n was in the range from 0.48993 to 0.8752 for the samples prepared by solution cast method and in the range from 0.861 to 0.90475 for the samples prepared by the electrospinning method. These results reveal the semiconductor behaviors of the composites [44]. It is evident from the results that none of the MWCNTs composites displayed the ideal dielectric behavior exhibited by the pure PVDF/PAN; however, the samples ranged from pure dielectric to clear semiconductor behavior as the content of MWCNTs in the material decreased. For very thin samples (for example, 1 mm), the frequency independence of the impedance modulus is suggestive of an ohmic material that must exhibit a very well-connected nanotube network. When the loading of the MWCNTs in the material increased, it appeared that the uniformity of materials started playing a more significant role which made it difficult for the nanotubes to arrange themselves into an interconnected 3D net.

The relationship between the electrical conductivity of the PVDF-PAN/MWCNTs composites and the temperature is on display in Fig. 6. As seen in Fig. 6, the electrical conductivity of the composites increased with temperature. The conductivity of the nanocomposites were analyzed according to the well-known Arrhenius equation [45]:

$$\sigma = \sigma_o \, \exp \left[\frac{-E_a}{k \, T} \right] \qquad (2)$$

Where E_a is the conductivity activation energy, k is the Boltzman constant and σ_o is the pre-exponential factor, which

Table 1 Arrhenius activation parameters for the PVDF-PAN/MWCNTs prepared by the electrospinning method and the solution cast method

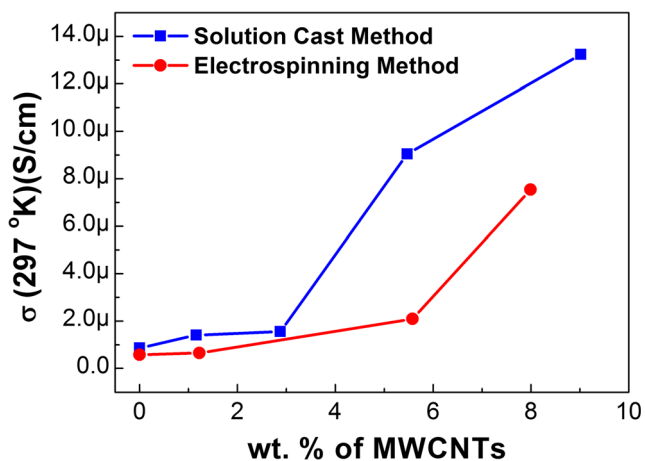| Electrospinning method			Solution cast method		
Wt.% of MWCNTs	σ_o [mS/cm]	E_a [meV]	Wt.% of MWCNTs	σ_o [mS/cm]	E_a [meV]
0	0.045	112	0	6.61	127
1.22	0.333	161	1.16	0.165	121
5.58	0.0046	20.5	2.88	0.311	135
7.99	5.36	166	5.47	0.027	282
			9.02	5.92	158

includes the charge carrier mobility and density of state. The semilogarithmic plots of $\ln(\sigma)$ vs. T^{-1} are linear with conductivity activation energy, E_a, values of 112 and 282 meV for PVDF/PAN and PVDF-PAN/MWCNTs, respectively.

The corresponding values of the activation energies are in Table 1. It clearly showed that the electrical conductivity of PVDF-PAN/MWCNTs, prepared by the electrospinning method, increased from 5.7×10^{-7} S/cm to 1.31×10^{-5} S/cm with the increase of MWCNTs content. On the other hand, when the content of MWCNTs in the nanocomposites increased, the electrical conductivity of PVDF-PAN/MWCNTs prepared by the solution cast method increased from 8.6×10^{-7} to 2.33×10^{-5} S/cm.

Figure 7 presents the conductivity of PVDF-PAN/MWCNTs composites prepared by using electrospinning and solution cast methods as a function of the MWCNTs contents. The electrical conductivity as a function of MWNTs showed the order of 5.7×10^{-7} S/cm to 1.23×10^{-6} S/cm at 24 °C. The conductivity of PVDF-PAN/MWCNTs was compared using the electrospinning method and the solution cast
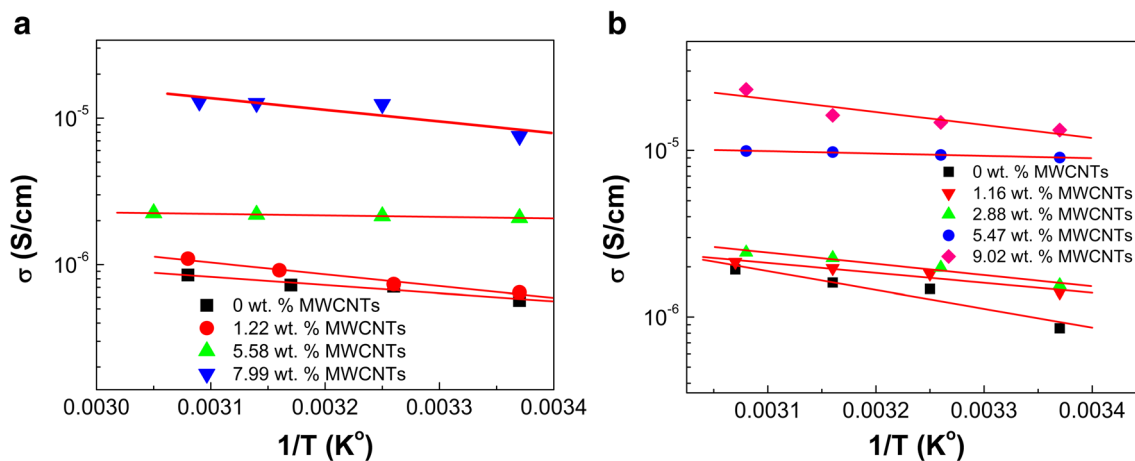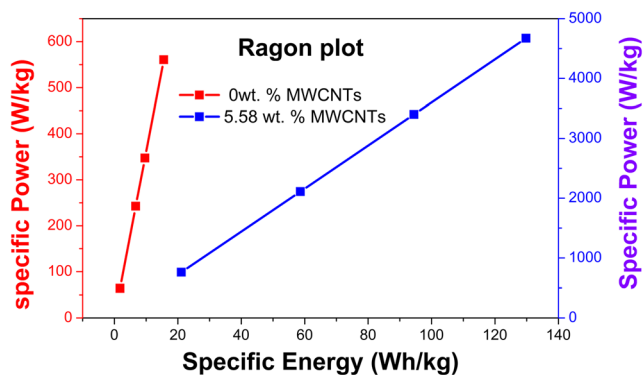

Fig. 6 Arrhenius plots of the PVDF-PAN/MWCNTs composites prepared by electrospinning method (**a**) and prepared by solution cast method (**b**) with different content of MWCNTs

Fig. 7 Electrical conductivity of the PVDF-PAN/MWCNTs composites as a function of the MWNT content

Fig. 9 Plot of specific power vs. specific energy (Ragon plots) for PVDF-PAN/MWCNTs composite (prepared by electrospinning method)

method at the same wt.%. The conductivity by the solution cast method had a higher conductivity (9.18×10^{-6} S/cm) than the conductivity by the electrospinning method (2.09×10^{-6} S/cm). Similar results were reported by Yu et al. [46]. It was determined that the electrical conductivity of pristine SWCNTs/epoxy composites were several orders higher than that of carboxylic functionalized SWCNTs/epoxy composites with the same SWCNTs content.

It was observed that the addition of MWCNTs into PVDF/PAN could enhance the conductivity of the studied polymer with an increased MWCNTs percentage; however, the phase transformation encouraged a change of conduction mechanism. The polymer nanocomposites with a high α-phase demonstrated a clear percolating behavior on the measured conductivity with high values for the percolation threshold. By the electrostatic interaction of functional groups on the MWCNTs with the polar-CF$_2$, the PVDF chain will have the zig-zag conformation of the β-phase, instead of the coiled α-phase

conformation. The polymer nanocomposites with high β-phase exhibits typical ionic conduction behavior due to the breaking of percolation paths associated to the structural and morphological changes. The obtained electronic parameters prove that PVDF-PAN/MWCNTs exhibit organic semiconductor behavior. In particular, compared with other spherical-shaped conductive filling materials such as carbon black, MWCNTs with large length/diameter aspect ratios help the composite system show a high electric conductivity at low concentrations due to their low percolation threshold [47, 48]. However, Carabineiro et al. [49] observed that the conductivity of the PVDF-MWCNTs further increased by nearly three orders of magnitude, from order of 10^{-7} S/cm to order of 10^{-4} S/cm, by the increased concentration of the MWCNTs.

Figure 8 shows typical galvanostatic discharge of PVDF-PAN/MWCNTs with different currents and wt.% of MWCNTs. It showed that the potential decreased exponentially, nearly to zero. The discharge time of polymer nanocomposites increased with the increase of MWCNTs content.
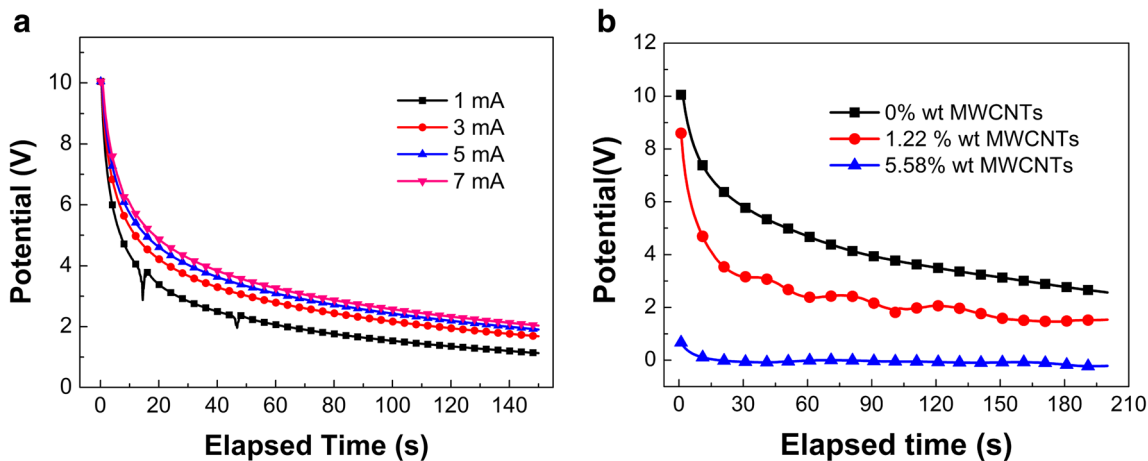
Fig. 8 Galvanostatic discharge of PVDF-PAN/MWCNTs prepared by electrospinning method (**a**) and prepared by electrospinning method (**b**) at different currents and different wt.% of MWCNTs

Galvanostatic discharge curves (Figs. 8a, b) were used to determine the capacitance of the polymer composite electrodes. The specific capacitance per mass of one pellet electrode was calculated according to the equation:

$$C_{sp} = \frac{I \times \Delta t}{\Delta E \times m} \tag{3}$$

where I is the discharge current in amperes, Δt is the discharge time in seconds corresponding to the voltage difference ΔE in volts, and m is the mass in grams. It was found that the specific capacitance increased from 0.2 to 8 F/g by increasing the current density and wt.% of MWCNTs. The specific power (SP) and specific energy (SE) were calculated from charge-discharge cycling data using the following relationships [50]:

$$Specific \quad Power \left(\frac{W}{kg} \right) = \frac{I \times \Delta E}{m} \tag{4}$$

$$Specific \quad Energy \left(\frac{Wh}{kg} \right) = \frac{I \times \Delta E \times t}{m \times 3600} \tag{5}$$

where I, t, and m are the discharge current in amperes, discharge time in seconds, and mass of PVDF-PAN/MWCNTs in kg, respectively. The calculated SP and SE values are shown in Fig.9 (Ragon plot). It is found that the largest specific energy for PVDF/PAN of 15.57 Wh/kg was obtained at a corresponding specific power of 560.3 W/kg and the largest specific energy for PVDF-PAN/MWCNTs (with 5.58 wt.% of MWCNTs) of 129.7 Wh/kg was obtained at a corresponding specific power of 4671 W/kg.

It was noticed that the specific energy of the PVDF-PAN/MWCNTs increased from 15.57 Wh/kg to 129.7 Wh/kg after the addition of MWCNTs. It was several times higher than that of the polymer blend without MWCNTs. It is clear that the PVDF-PAN/MWCNTs have high-performance electronic components. These characteristic properties of obtained polymer nanocomposites will prove to be optimal candidates for many applications such as nanogenerators, organic semiconductors, transducers, and electrical energy storage [51].

4 Conclusions

PVDF/PAN/MWCNTs nanocomposites with different contents of MWCNTs were successfully prepared through electrospinning and the solution cast method. FTIR results indicate that MWCNTs act as a nucleation agent during crystallization and slightly increased the β-phase crystal and could decrease the α-phase in the PVDF/ PAN/MWCNTs-COOH nanocomposites. The morphological properties and electrical conductivity of polymer nanocomposites have been analyzed. The results showed that the nanocomposites prepared by the solution cast method had a much higher conductivity

$(9.18 \times 10^{-6}$ S/cm) than those prepared by the electrospinning method $(2.09 \times 10^{-6}$ S/cm) at the same MWCNTs content. In conclusion, the MWCNTs play a very important role in both structural and electrical properties of the composites. The polymer nanocomposites can be useful for applications such as nanogenerators, organic semiconductors, transducers, and electrical energy storage.

References

1. Stankovich S, Dikin DA, Dommett GH, Kohlhaas KM, Zimney EJ, Stach EA, Piner RD, Nguyen ST, Ruoff RS (2006) Graphene-based composite materials. Nature 442(7100):282–286
2. Wu M, Shaw L (2006) Electrical and mechanical behaviors of carbon nanotube-filled polymer blends. J Appl Polym Sci 99(2):477–488
3. Yuen SM, Ma CCM, Chiang CL, Lin YY, Teng CC (2007) Preparation and morphological, electrical, and mechanical properties of polyimide-grafted MWCNT/polyimide composite. J Polym Sci A Polym Chem 45(15):3349–3358
4. Aqeel SM, Küçükyavuz Z (2011) Characterization and electrical conductivity of poly (ethylene glycol)/polyacrylonitrile/multiwalled carbon nanotube composites. J Appl Polym Sci 119(1):142–147
5. Aqeel SM, Wang Z, Than L, Sreenivasulu G, Zeng X (2015) Poly (vinylidene fluoride)/poly (acrylonitrile)–based superior hydrophobic piezoelectric solid derived by aligned carbon nanotubes in electrospinning: fabrication, phase conversion and surface energy. RSC Adv 5(93):76383–76391
6. Wang Z, Colorad HA, Guo Z-H, Kim H, Park C-L, Hahn HT, Lee S-G, Lee K-H, Shang Y-Q (2012) Effective functionalization of carbon nanotubes for bisphenol F epoxy matrix composites. Mater Res 15(4):510–516
7. Agarwal A, Bakshi SR, Lahiri D (2016) Carbon nanotubes: reinforced metal matrix composites. CRC press
8. Wang Z, Lu M, Li H-L, Guo X-Y (2006) SWNTs–polystyrene composites preparations and electrical properties research. Mater Chem Phys 100(1):77–81
9. Zhang L, Zhang Q, Xie H, Guo J, Lyu H, Li Y, Sun Z, Wang H, Guo Z (2017) Electrospun titania nanofibers segregated by graphene oxide for improved visible light photocatalysis. Appl Catal B Environ 201:470–478
10. Wei H, Cui D, Ma J, Chu L, Zhao X, Song H, Liu H, Liu T, Wang N, Guo Z (2017) Energy conversion technologies towards self-powered electrochemical energy storage systems: the state of the art and perspectives. J Mater Chem A
11. Huang B, Wang Z, Chen L, Xue R, Wang F (1996) The mechanism of lithium ion transport in polyacrylonitrile-based polymer electrolytes. Solid State Ionics 91(3):279–284
12. Tatsuma T, Taguchi M, Iwaku M, Sotomura T, Oyama N (1999) Inhibition effects of polyacrylonitrile gel electrolytes on lithium dendrite formation. J Electroanal Chem 472(2):142–146

13. Nalwa HS (1995) Ferroelectric polymers: chemistry: physics, and applications. CRC Press, Boca Raton

14. Ducharme S, Reece TJ, Othon CM, Rannow RK (2005) Ferroelectric polymer Langmuir-Blodgett films for nonvolatile memory applications. IEEE Trans Device Mater Reliab 5(4):720–735

15. Naber RC, Asadi K, Blom PW, de Leeuw DM, de Boer B (2010) Organic nonvolatile memory devices based on ferroelectricity. Adv Mater 22(9):933–945

16. Guan F, Pan J, Wang J, Wang Q, Zhu L (2009) Crystal orientation effect on electric energy storage in poly (vinylidene fluoride-co-hexafluoropropylene) copolymers. Macromolecules 43(1):384–392

17. Guan F, Yuan Z, Shu EW, Zhu L (2009) Fast discharge speed in poly (vinylidene fluoride) graft copolymer dielectric films achieved by confined ferroelectricity. Appl Phys Lett 94(5):052907

18. Sreekumar TV, Liu T, Min BG, Guo H, Kumar S, Hauge RH, Smalley RE (2004) Polyacrylonitrile single-walled carbon nanotube composite fibers. Adv Mater 16(1):58–61

19. Ko F, Gogotsi Y, Ali A, Naguib N, Ye H, Yang G, Li C, Willis P (2003) Electrospinning of continuous carbon nanotube-filled nanofiber yarns. Adv Mater 15(14):1161–1165

20. Prilutsky S, Zussman E, Cohen Y (2010) Carbonization of electrospun poly (acrylonitrile) nanofibers containing multiwalled carbon nanotubes observed by transmission electron microscope with in situ heating. J Polym Sci B Polym Phys 48(20):2121–2128

21. Huang J, Cao Y, Huang Z, Imbraguglio SA, Wang Z, Peng X, Guo Z (2016) Comparatively Thermal and Crystalline Study of Poly (methyl-methacrylate)/Polyacrylonitrile Hybrids: Core–Shell Hollow Fibers, Porous Fibers, and Thin Films. Macromol Mater Eng 301(11):1327–1336

22. Guan X, Zheng G, Dai K, Liu C, Yan X, Shen C, Guo Z (2016) Carbon nanotubes-adsorbed electrospun PA66 nanofiber bundles with improved conductivity and robust flexibility. ACS Appl Mater Interfaces 8(22):14150–14159

23. Ghafari E, Feng Y, Liu Y, Ferguson I, Lu N (2017) Investigating process-structure relations of ZnO nanofiber via electrospinning method. Compos Part B 116:40–45

24. Heikkilä P, Harlin A (2008) Parameter study of electrospinning of polyamide-6. Eur Polym J 44(10):3067–3079

25. Huang Z-M, Zhang Y-Z, Kotaki M, Ramakrishna S (2003) A review on polymer nanofibers by electrospinning and their applications in nanocomposites. Compos Sci Technol 63(15):2223–2253

26. Varesano A, Carletto RA, Mazzuchetti G (2009) Experimental investigations on the multi-jet electrospinning process. J Mater Process Technol 209(11):5178–5185

27. Kim JS, Reneker DH (1999) Polybenzimidazole nanofiber produced by electrospinning. Polym Eng Sci 39(5):849–854

28. Fang X, Reneker D (1997) DNA fibers by electrospinning. J Macromol Sci Part B: Phys 36(2):169–173

29. Park SJ, Cho MS, Lim ST, Choi HJ, Jhon MS (2005) Electrorheology of multiwalled carbon nanotube/poly (methyl methacrylate) nanocomposites. Macromol Rapid Commun 26(19):1563–1566

30. Dong H, Nyame V, MacDiarmid AG, Jones WE (2004) Polyaniline/poly (methyl methacrylate) coaxial fibers: The fabrication and effects of the solution properties on the morphology of electrospun core fibers. J Polym Sci B Polym Phys 42(21):3934–3942

31. Gopalan AI, Santhosh P, Manesh KM, Nho JH, Kim SH, Hwang C-G, Lee K-P (2008) Development of electrospun PVdF–PAN membrane-based polymer electrolytes for lithium batteries. J Membr Sci 325(2):683–690

32. Yu H, Huang T, Lu M, Mao M, Zhang Q, Wang H (2013) Enhanced power output of an electrospun PVDF/MWCNTs-based nanogenerator by tuning its conductivity. Nanotechnology 24(40):405401

33. Sahoo NG, Bao H, Pan Y, Pal M, Kakran M, Cheng HKF, Li L, Tan LP (2011) Functionalized carbon nanomaterials as nanocarriers for loading and delivery of a poorly water-soluble anticancer drug: a comparative study. Chem Commun 47(18):5235–5237

34. Trchová M, Šeděnková I, Tobolková E, Stejskal J (2004) FTIR spectroscopic and conductivity study of the thermal degradation of polyaniline films. Polym Degrad Stab 86(1):179–185

35. Vasundhara K, Mandal BP, Tyagi AK (2015) Enhancement of dielectric permittivity and ferroelectricity of a modified cobalt nanoparticle and polyvinylidene fluoride based composite. RSC Adv 5(12):8591–8597

36. Song R, Yang D, He L (2007) Effect of surface modification of nanosilica on crystallization, thermal and mechanical properties of poly (vinylidene fluoride). J Mater Sci 42(20):8408–8417

37. He L, Sun J, Wang X, Yao L, Li J, Song R, Hao Y, He Y, Huang W (2011) Enhancement of β-crystalline phase of poly (vinylidene fluoride) in the presence of hyperbranched copolymer wrapped multiwalled carbon nanotubes. J Colloid Interface Sci 363(1):122–128

38. Bao S, Liang G, Tjong SC (2011) Effect of mechanical stretching on electrical conductivity and positive temperature coefficient characteristics of poly (vinylidene fluoride)/carbon nanofiber composites prepared by non-solvent precipitation. Carbon 49(5):1758–1768

39. Zhong G, Zhang L, Su R, Wang K, Fong H, Zhu L (2011) Understanding polymorphism formation in electrospun fibers of immiscible poly (vinylidene fluoride) blends. Polymer 52(10):2228–2237

40. Gao Q, Scheinbeim JI (2000) Dipolar intermolecular interactions, structural development, and electromechanical properties in ferroelectric polymer blends of nylon-11 and poly (vinylidene fluoride). Macromolecules 33(20):7564–7572

41. Almond D, West A (1987) The activation entropy for transport in ionic conductors. Solid State Ionics 23(1):27–35

42. Jonscher AK (1977) Theuniversal'dielectric response. Nature 267:673–679

43. Barik SK, Choudhary R, Singh A (2011) Ac impedance spectroscopy and conductivity studies of Ba0. 8Sr0. 2TiO3 ceramics. Adv Mater Lett 2(6):419–424

44. Kim D, Kim Y, Choi K, Grunlan JC, Yu C (2009) Improved thermoelectric behavior of nanotube-filled polymer composites with poly (3, 4-ethylenedioxythiophene) poly (styrenesulfonate). ACS Nano 4(1):513–523

45. Kang SD, Snyder GJ (2016) Charge-transport model for conducting polymers. Nat Mater 2: 252

46. Yu A, Itkis ME, Bekyarova E, Haddon RC (2006) Effect of single-walled carbon nanotube purity on the thermal conductivity of carbon nanotube-based composites. Appl Phys Lett 89(13):133102

47. Du J, Zhao L, Zeng Y, Zhang L, Li F, Liu P, Liu C (2011) Comparison of electrical properties between multi-walled carbon nanotube and graphene nanosheet/high density polyethylene composites with a segregated network structure. Carbon 49(4):1094–1100

48. Kovacs JZ, Velagala BS, Schulte K, Bauhofer W (2007) Two percolation thresholds in carbon nanotube epoxy composites. Compos Sci Technol 67(5):922–928

49. Carabineiro S, Pereira M, Nunes-Pereira J, Silva J, Caparrós C, Sencadas V, Lanceros-Méndez S (2012) The effect of nanotube surface oxidation on the electrical properties of multiwall carbon nanotube/poly (vinylidene fluoride) composites. J Mater Sci 47(23):8103–8111

50. Reddy ALM, Ramaprabhu S (2007) Nanocrystalline metal oxides dispersed multiwalled carbon nanotubes as supercapacitor electrodes. J Phys Chem C 111(21):7727–7734

51. Wang Q, Zhu L (2011) Polymer nanocomposites for electrical energy storage. J Polym Sci B Polym Phys 49(20):1421–1429